Molecular Omics

ROYAL SOCIETY OF CHEMISTRY

RESEARCH ARTICLE

View Article Online
View Journal | View Issue

Cite this: *Mol. Omics*, 2020, **16**, 345

Mycobacterium bovis BCG infection alters the macrophage *N*-glycome†

Clément Delannoy,‡[a] Chin Huang,‡[bc] Bernadette Coddeville,[a] Jian-You Chen,[b] Dounia Mouajjah,[a] Sophie Groux-Degroote,[a] Anne Harduin-Lepers,[a] Kay-Hooi Khoo,[b] Yann Guerardel*[a] and Elisabeth Elass-Rochard[a]

Macrophage glycosylation is essential to initiate the host-immune defense but may also be targeted by pathogens to promote infection. Indeed, the alteration of the cell-surface glycosylation status may affect the binding of lectins involved in cell activation and adhesion. Herein, we demonstrate that infection by *M. bovis* BCG induces the remodeling of the *N*-glycomes of both human primary blood monocyte-derived macrophages (MDM) and macrophage-cell line THP1. MALDI-MS based *N*-glycomic analysis established that mycobacterial infection induced increased synthesis of biantennary and multifucosylated complex type *N*-glycans. In contrast, infection of macrophages by *M. bovis* BCG did not modify the glycosphingolipids composition of macrophages. Further nano-LC-MS^n glycotope-centric analysis of total *N*-glycans demonstrated that the increased fucosylation was due to an increased expression of the Le^x (Galβ1-4[Fucα1-3]GlcNAc) epitope, also known as stage-specific embryonic antigen-1. Modification of the surface expression of Le^x was further confirmed in both MDM and THP-1 cells by FACS analysis using an α1,3-linked fucose specific lectin. Activation with the mycobacterial lipopeptide Pam3Lp19, an agonist of toll-like receptor 2, did not modify the overall fucosylation pattern, which suggests that the infection process is required to modify surface glycosylation. These results pave the way toward the understanding of infection-triggered cell-surface remodeling of macrophages.

Received 27th November 2019,
Accepted 30th March 2020

DOI: 10.1039/c9mo00173e

rsc.li/molomics

Introduction

The glycome of immune cells comprises a wide variety of glycans carried on secreted and membrane-associated proteins and lipids,[1,2] and is fundamental to initiating proper host defense.[3–5] It is now well-appreciated that the biological activities of various glycosylated immune molecules such as the immune receptors (toll-like receptors, mannose-receptor), IgG antibodies, cytokines, integrins and ligands of selectins are dependent on their glycosylation status.[6–8] Significant glycome changes are noted in a wide range of pathological states including cancer,[3] inflammatory diseases,[9] and bacterial infection,[10,11] and are often positively correlated with regulated expression of glycosyltransferase (GT) genes. In particular, alterations in both the terminal capping and elongation of glycans may affect the interaction of cells with host immune lectins, such as selectins and galectins that transduce a multitude of functional effects including modulation of cell activation, survival and migration, or microbial lectins that mediate adhesion of pathogens.[12] In turn, bacteria may manipulate host glycosylation to their own benefit. Several of these microorganisms invade macrophages, in which they multiply and further control numerous cell-signaling pathways including production of cytokines and reactive oxygen species, fusion of phagosomes with lysosomes, cell apoptosis and autophagy.[13–15] Modulated ion of gene expressions of galactosyltransferases, sialyltransferases, neuraminidases and fucosidases in macrophages exposed to *Mycobacterium tuberculosis* (Mtb) have been reported.[16,17] Alteration of sialylation was also detected in murine macrophages activated with purified mycobacterial cell wall glycolipids, such as trehalose-dimycolate (TDM).[18,19] Here, we have investigated by a mass spectrometry approach to what extent *M. bovis* BCG modulates the glycome of infected human primary blood monocyte-derived macrophages (MDM) and macrophage-like THP-1 cells, both commonly used as relevant cell models to study immunomodulatory functions of infected phagocytes.[20,21] Our in depth analysis revealed a significantly increased expression of terminal fucosylated epitope, Le^x, carried on complex type *N*-glycans, while the glycosphingolipid (GSL) profiles remained largely unaffected.

[a] *Univ. Lille, CNRS UMR 8576, UGSF-Unité de Glycobiologie Structurale et Fonctionnelle, 59 000 Lille, France. E-mail: yann.guerardel@univ-lille.fr*
[b] *Institute of Biological Chemistry, Academia Sinica, Taiwan*
[c] *Department of Biochemical Sciences and Technology, National Taiwan University, Taiwan*

† Electronic supplementary information (ESI) available. See DOI: 10.1039/c9mo00173e
‡ These authors have contributed equally to the work.

Experimental

Cell culture

Differentiated THP-1 cells. Human monocytic THP-1 leukemia cells (ECACC no. 88081201) were differentiated into macrophage-like cells with 20 nM phorbol-12-myristate-13-acetate (PMA) for 72 h, in RPMI-1640 medium supplemented with 10% (v/v) heat-inactivated FCS, 2 mM L-glutamine and 20 μM β-mercaptoethanol, as previously described.[22,23] Non-adherent cells were removed by washing with Phosphate Buffered Saline (PBS).

Human primary blood monocyte-derived macrophages (MDM). Human blood samples from healthy donors were collected at the local blood transfusion center (Etablissement Français du Sang, Lille). Peripheral blood mononuclear cells (PBMC) were isolated by Ficoll density gradient centrifugation (Lymphoprep, AbCys). Monocytes were purified from PBMC by immunomagnetic selection with magnetic beads coupled to CD14, according to the instructions of the manufacturer (Miltenyi Biotech). The monocyte preparations were more than 95% pure, as checked by flow cytometry. MDM were obtained by incubating freshly isolated monocytes (10^6 cells per mL) in complete RPMI 1640, 10% (v/v) FCS supplemented with 10 ng mL^{-1} GM-CSF, for 6 days, as previously described in the literature.[24] Fresh medium with GM-CSF was added after 2 and 4 days.

Mycobacterial cell culture and infection

M. bovis BCG (Pasteur strain) was obtained from Pasteur Institute (Lille, France). Mycobacteria were grown in Sauton medium on a shaker at 37 °C. The Sauton medium was prepared as described by Larsen and collaborators.[25]

After 6 days of monocyte differentiation into M_0, macrophage adherent cells were infected with *M. bovis* BCG at MOI 5 : 1 (5 mycobacteria per macrophage) or activated by 0.5 μg mL^{-1} of mycobacterial lipopeptide PAM_3Lp_{19} and maintained in a humidified atmosphere with 5% (v/v) CO_2 at 37 °C for 48 h.[26,27] The activation of differentiated THP-1 cells was performed in similar conditions.

Flow cytometry analysis of cell surface markers during cell activation

The activation of both PMA THP-1 cells and MDM, by either BCG-infection or lipopeptide stimulation, was controlled by measuring the cell surface antigen expression (CD80, CD40, and CD54) in unstimulated and activated cells by flow cytometry. First, cells were pre-incubated for 20 min at 4 °C with Fc-receptor blocking reagent (Innovex Biosciences, Richmond, CA, USA) to decrease the non-specific binding of immunoglobulin to the cells. Cell surface immunostaining was directly applied for 40 min at 4 °C in PBS/0.1% (w/v) BSA with fluorescein-conjugated mouse anti-human CD80, anti-CD40 Abs or PE-conjugated mouse anti-CD54 (BD Biosciences, Le Pont de Claix, France). FITC- or PE-conjugated mouse isotype control IgG (BD Biosciences) was used as a negative control. Data were monitored on a flow cytofluorimeter (FACSCalibur, BD Biosciences) and analyzed with the CellQuest software (Mountain View, CA, USA).

Quantitation of pro-inflammatory cytokine secretion by ELISA

After 8 h or 24 h activation, culture supernatants were collected and analyzed for the detection of TNF-α and IL-1β, respectively, by sandwich ELISA, according to the manufacturers' instructions (Ozyme S.A.). Cytokine concentrations were determined using standard curves obtained with recombinant human TNF-α or IL-1β. The statistical significance was determined using the Student t test, with GraphPad Prism 5 (only values of $p < 0.05$ were considered to be significant).

Glycolipid extraction and purification

Infected or uninfected cells were detached from T75 flasks with cell dissociation non-enzymatic solution and washed twice with PBS. The cells (5×10^6) were lyophilized and extracted three times with $CHCl_3/CH_3OH$ (2 : 1, v/v) and once with $CHCl_3/CH_3OH$ (1 : 2, v/v) using intermediary centrifugations at 2500*g* for 20 min. The combined supernatants were dried under a nitrogen stream, subjected to mild saponification in 0.1 M NaOH in $CHCl_3/CH_3OH$ (1 : 1, v/v) at 37 °C for 2 h and evaporated to dryness. The samples were reconstituted in CH_3OH/0.1% TFA in water (1 : 1, v/v) and applied to a reverse phase C_{18} cartridge (Waters, Milford, MA, USA) equilibrated in the same solvent. After washing with CH_3OH/0.1% TFA in water (1 : 1, v/v), GSL were eluted with CH_3OH, $CHCl_3/CH_3OH$ (1 : 1, v/v) and $CHCl_3/CH_3OH$ (2 : 1, v/v). The elution fraction was dried under a nitrogen stream prior to structural analysis.

Release and purification of *N*-glycans

Cells were resuspended with Triton X-100 extraction buffer (1% Triton X-100 in PBS buffer). To lyse the cells, the suspension was sonicated for 30 min. Debris and the insoluble fraction were pelleted down by centrifugation at 13 000 rpm for 10 min at 4 °C, and the supernatant was kept. A 1/10 volume of 0.1 M dithiothreitol was added to a final concentration of 10 mM and incubated at 37 °C for 1 hour, followed by addition of a 1/10 volume of 0.5 M iodoacetamide for 1 hour in the dark at 37 °C. The reduced/alkyled glycoproteins were precipitated with a 1/9 volume of trichloroacetic acid to final 10% (v/v) at −20 °C for 30 min. The pellet was precipitated by centrifugation at 13 000 rpm for 10 min at 4 °C, and then the supernatant was discarded. The pellet was resuspended and washed with 1 mL of cold acetone, and then centrifuged at 13 000 rpm for 10 min at 4 °C, and this step was repeated three times. The sample was incubated with trypsin (Sigma-Aldrich) in 50 mM NH_4HCO_3, pH 8.4, overnight at 37 °C. The reaction was quenched by boiling at 100 °C for 5 min. *N*-Glycans were released by *N*-glycosidase F (BioLabs) digestion at 37 °C for 1 day and *N*-glycans and *O*-glycopeptides were separated by C_{18} Sep-Pak chromatography. C_{18} Sep-Pak was equilibrated in 5% (v/v) aqueous acetic acid and washed in the same solvent. The sample was loaded on the C_{18} Sep-Pak and the released *N*-glycans were eluted with 5% (v/v) aqueous acetic acid and the bound peptides with 20%,

40% and 60% (v/v) propanol in 5% aqueous acetic acid, pooled and lyophilized.

Mass spectrometry analysis of glycans

Glycans and glycolipids were permethylated according to the method of Ciucanu and Kerek[28] prior to mass spectrometry analysis. Briefly, the samples were incubated with DMSO/NaOH/ICH_3 for 2 h under agitation. The derivatization was stopped by addition of water and the permethylated glycans were extracted in $CHCl_3$ and washed at least seven times with water. Then, the permethylated *N*-glycans were purified on C_{18} Sep-Pak. The samples were washed with ACN/0.1% (v/v) TFA in water (1 : 9, v/v) and eluted with ACN/0.1% TFA in water (8 : 2, v/v). The permethylated glycans were solubilized in ACN/H_2O (1 : 1, v/v) and mixed with 2,5-dihydroxybenzoic acid matrix solution (10 mg mL^{-1}) dissolved in ACN/H_2O (1 : 1, v/v) and spotted on a MALDI plate. MALDI-TOF and MALDI-TOF/TOF spectra were acquired using a 4800 TOF/TOF spectrometer (Applied Biosystems, Framingham, MA, USA) in reflectron positive mode. The laser was set at 337 nm and a frequency of 200 Hz with 5000 shots per spot was used for MS and MS/MS data acquisition.

Additional permethylated glycan samples were analyzed by nanoLC-MS/MS on an Orbitrap Fusion Tribrid system (ThermoFisher Scientific), using the same reverse phase C_{18} nanoLC conditions, instrument settings, MS^2-product dependent MS^3 data acquisition, processing and analysis methods described previously.[29] To identify potential changes in α2-3 *vs.* 2-6-sialylation, the released glycan samples were subjected to dimethylamidation prior to permethylation[30] and mapped against the non-dimethylamidated samples first by MALDI-MS on a MALDI TOF/TOF 5800 system (AB Sciex) and then by nanoLC-MS/MS analyses. Dimethylamidation was performed by adding 25 μL of freshly prepared reagent containing 250 mM EDC, 500 mM HOBt, and 250 mM dimethylamine in DMSO to the glycan samples and incubated at 60 °C for 1.5 h. After drying, the samples were cleaned by passing through C_{18} Sep-Pak cartridges equilibrated in 5% (v/v) acetic acid before being subjected to permethylation.

Detection of carbohydrate epitopes by flow cytometry

To detect the variation of fucosylated epitopes at the cell surface of activated macrophages, the binding of FITC-conjugated plant lectins, such as LTA (*Lotus tetranologobus* agglutinin) and UEA-I (*Ulex europaeus* I agglutinin), which have specificity for α-L-fucose was investigated by flow cytometry.[31,32] Untreated and infected cells (250 000 per well) were incubated with each lectin at 15 μg mL^{-1} for 40 min at 4 °C in PBS with calcium and magnesium containing 0.05% (w/v) BSA which has been previously pretreated by sodium metaperiodate. Furthermore, the non-specific binding of LTA and UEA-I to cells was evaluated in the presence of α L-fucose. After washing, fluorescence analysis was performed on a FACSCalibur, as previously described above. The log of the fluorescence intensities in arbitrary units is plotted against the cell number. For each lectin, the ratio of the mean fluorescence intensity (MFI) of stimulated cells *versus* the MFI of unactivated cells was determined from three independent experiments performed in triplicate, with MDM obtained from three blood donors. The statistical significance between the untreated and stimulated cells was determined using the Student *t* test. Values of $p < 0.05$ were considered to be significant.

Results and discussion

PMA-treated THP-1 cells and human primary monocyte-derived macrophages (MDM) were used as models of study because they are known to display similar phagocytic capacity toward *M. bovis* BCG, leading to up-regulation of the expression of cell surface markers and pro-inflammatory cytokine secretion.[20] Prior to glycome analysis, we have checked that macrophages (PMA THP-1 and MDM) infected by *M. bovis* BCG or incubated with the lipopeptide exhibited a pro-inflammatory phenotype through the increased expression of cell surface antigens and increased production of TNF-α and IL1-β (ESI,† Fig. S1).

GSL profiles

Glycosphingolipids were then extracted from THP-1 and purified by solid phase extraction (SPE) on a C_{18} cartridge and analysed by MALDI-MS in permethylated forms based on the calculated composition of glycan ceramide moieties and the prior knowledge of the biosynthetic pathways of human GSL (Fig. 1A). The MS/MS fragmentation analyses show that neutral GSL are composed of (iso)globosides (i)Gb3 (Galα1-3/4Galβ1-4Glcβ1-Cer) and Gb4 (GalNAcβ1-3Galα1-3/4Galβ1-4Glcβ1-Cer), as well as neutral ganglioside GA1 substituted by major ceramides [d18:1-C16:0 (Cer*)] and [d18:1-C24:0 (Cer**)] (ESI,† Fig. S2C). Among sialylated GSL, ganglioside GM3 (Neu5Acα2-3Galβ1-4Glcβ1-Cer) is the major structure, but other sialylated structures such GM1, GD3 and GD1a were also detected. Infection by *M. bovis* BCG and activation by the lipopeptide PAM_3-Lp_{19} did not modify the GSL patterns of THP1 cells (Fig. 1B and ESI,† Fig. S2A and B). Compared to PMA THP-1, MDM exhibited a much simpler GSL profile, dominated by GM3 associated with [d18:1/C16:0 (Cer*)] and [d18:1/C24:1 (Cer**)] (Fig. 1C), with traces of GM1 in some batches of MDM. As observed for PMA THP-1, *M. bovis* BCG infection did not induce any modification of the GSL profiles of MDM (ESI,† Fig. S3).

N-Glycan profiles

The *N*-glycans isolated from THP-1 and MDM cells were similarly profiled by MALDI-MS analysis of permethylated derivatives (Fig. 2A and 3A). The nature of individual *N*-glycans was inferred based on their calculated composition and prior knowledge of the biosynthetic pathways of *N*-glycans (ESI,† Table S1). In both cell types, the lower mass range signals (*m*/*z* 1500 to 2500) were dominated by high-mannose *N*-glycans that represent more than 50% of the total *N*-glycans. The remaining compounds were identified as complex-type *N*-glycans differently sialylated, branched and fucosylated (Fig. 2A and 3A and ESI,† Table S1). The relative amounts of individual *N*-glycan signals were calculated by integrating their intensities for each condition

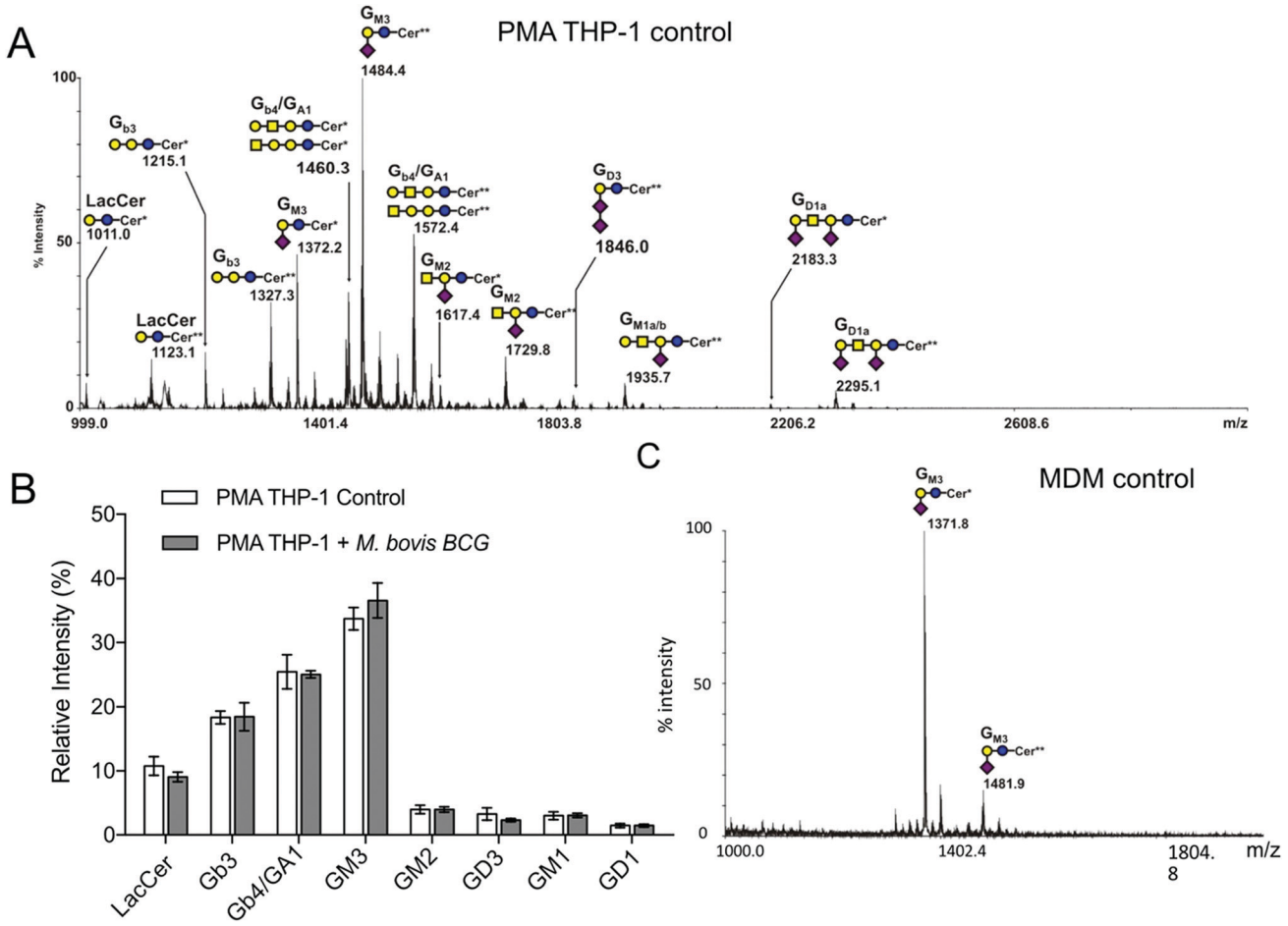

Fig. 1 Mass spectrometry analysis of glycosphingolipids extracted from macrophages. Representative MALDI-TOF-MS spectra (3 different experiments) of permethylated glycosphingolipids isolated from (A) PMA-THP-1 and (C) MDM cells. (B) Relative quantification of individual GLS species extracted from PMA-THP-1 cells prior to and after infection with *M. bovis* BCG. GSL are present as d18:1/C16:0 (Cer*) and d18:1/C24:0 (Cer**) isomers. The glycosyl composition assignment here was based on the detected mass values for the $[M + Na]^+$ molecular ions and annotated using the standard symbol nomenclature for glycan systems.[42]

and first computed according to their nature (high mannose or complex). After infection by *M. bovis* BCG, PMA THP-1 and MDM did not show significant variation in the ratio of high mannose type *versus* complex type *N*-glycans. Then, relative amounts of individual complex *N*-glycan signals were calculated by integrating their intensities and dividing them by the cumulated intensities of complex *N*-glycan signals, thus excluding high mannose *N*-glycans, and integrated into groups sharing similar features (Fig. 2B and 3B). Comparison of different groups showed that the prevalence of sialylation among complex type *N*-glycans in THP-1 and MDM was not significantly modified. To ascertain if there is any significant change in the α2,3/α2,6-sialyl linkages, the *N*-glycans from MDM cells were subjected to linkage-specific dimethylamide modifications prior to permethylation and MS analysis. Initial MALDI-MS profiling indicated that after dimethylamidation, most of the peaks assigned as sialylated complex type *N*-glycans were visibly accompanied by additional peaks at 13 u higher (ESI,† Fig. S4), consistent with the presence of the α2,6-sialyl linkage.[30] For signals carrying multiple sialic acids, multiple degrees of +13 u were observed, showing a variable degree of α2,6-sialylation. However, in all cases, a substantial amount of sialylated peaks remain unaffected, which indicates that sialylation on the *N*-glycans of MDM comprises both α2,3 and α2,6 linkages. Based on the relative intensities of the in source-generated oxonium ions at *m*/*z* 825 and 838 (ESI,† Fig. S5A), it could be further inferred that there are more α2,3 than α2,6 linkages but, most importantly, their relative amount was not appreciably affected upon *M. bovis* BCG treatment (ESI,† Fig. 5B).

Increased fucosylation

Contrary to the sialylation pattern, infection by *M. bovis* BCG induced reproducible variations (over four replicates of THP-1 cell cultures and three MDM donors) of antennae and fucosylation levels (Fig. 2B and 3B) on complex *N*-glycans. In MDM the proportion of mono- and multi-fucosylated *N*-glycans increases from 15 to 20% and from 12 to 17%, respectively. MALDI-MS/MS analysis of selected compounds showed that fucose residues could be attached to both the chitobiose core and LacNAc extensions of fucosylated *N*-glycans, as exemplified in the ESI,† Fig. S6. However, these analyses could not clearly

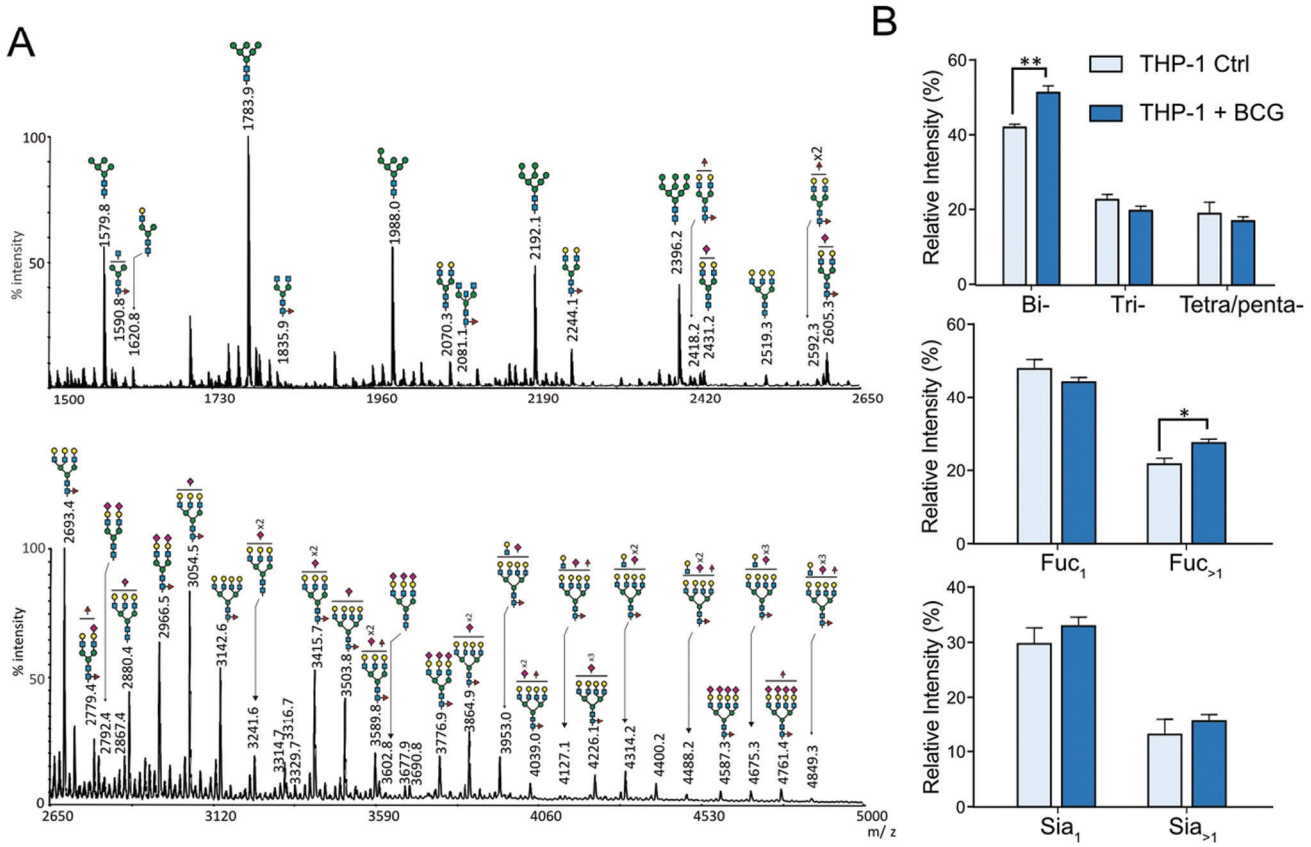

Fig. 2 MALDI-MS analyses of *N*-glycans isolated from THP1-cells. (A) MALDI-MS profile of permethylated *N*-glycans purified from uninfected PMA-differentiated THP-1 cells. The top panel shows the *m*/*z* 1500 to 2650 region and the lower panel shows the *m*/*z* 2650 to 5000 region of a single MALDI-MS spectrum. The compositions of major glycan signals were deduced from the *m*/*z* values of $[M + Na]^+$ adducts. The position of Fuc/Sia residues and branching patterns were not established at this stage and are only indicative. A complete list of identified *N*-glycans is provided in the ESI,† Table S1. (B) Differential profiling of complex *N*-glycans, extracted from PMA activated THP-1 cells, before (light blue) and after *M. bovis* BCG infection (deep blue). Top panel, proportions of multi-antennary complex-type *N*-glycans (bi, two LacNAc; tri, three LacNAc; tetra/penta, four and five LacNAc); middle panel, proportions of mono and multi-fucosylated complex type *N*-glycans; bottom panel, proportions of sialylated complex *N*-glycan. Relative intensities do not include oligomannosylated *N*-glycans. The statistical significance compared with untreated cells (**$p < 0.01$, *$p < 0.05$) was determined by a two-tailed *t*-test using GraphPad Prism 5 software. Data represent median ± interquartile range from 4 independent experiments from different cell cultures.

establish how the fucosylation pattern was modified following infection. In order to further delineate the nature and the extent of the glycosylation changes, we subjected the samples isolated from MDM cells to a semi-quantitative glycotope-centric glycomic mapping of total *N*-glycome.[29] Zooming in on fucosylated complex type *N*-glycans, it is clear that upon BCG treatment, not only were several mono-fucosylated peaks detected at slightly higher intensity than the non-fucosylated counterparts, but also those carrying a second Fuc (*m*/*z* 2508, 2795, 2883, 3244, 3833, 3419, and 3606) became more apparent (Fig. 4). The second Fuc was confirmed to be associated with terminal Hex-HexNAc by the oxonium ion at *m*/*z* 638, which was only produced in source fragmentation from the sample treated with BCG (Fig. 4). The detection of the range of terminal glycotopes by means of MALDI in source prompt fragmentation and the notable increase in fucosylation were corroborated by LC-MS/MS analysis of the permethylated sample under acidic conditions (ESI,† Fig. S7). Focusing only on the biantennary *N*-glycans that were better resolved, it is clear that those structures assigned as carrying 2 to 3 fucose residues were expressed at a higher level upon BCG treatment, after being normalized to the Man_9-high mannose peak (Fig. 4). Their structures were further verified by manually examining their respective HCD-MS^2 spectra (not shown), which produced the diagnostic MS^2 ion at *m*/*z* 638 ($Fuc_1Hex_1HexNAc^+$) and 825 ($NeuAc_1Hex_1HexNAc^+$) but not *m*/*z* 999 ($NeuAc_1Fuc_1Hex_1HexNAc^+$).

Increased Le^x expression

To resolve further the isomeric $Fuc_1Hex_1HexNAc_1$ glycotopes, the data dependent mode of MS^2 acquisition during the LC-MS/MS run was programmed to be coupled with product-dependent MS^3, targeting the MS^2 ion at *m*/*z* 638. In other words, whenever *m*/*z* 638 was detected among the MS^2 ions, it would be automatically taken through to an MS^3 event on the fly. Le^x would be unambiguously identified if the MS^3 ion at *m*/*z* 432 was detected. In addition to manually interpreting several of the MS^2/MS^3 spectra acquired, the entire range of distinctive glycotopes expressed in MDM with and without BCG treatment and their relative abundance were mapped

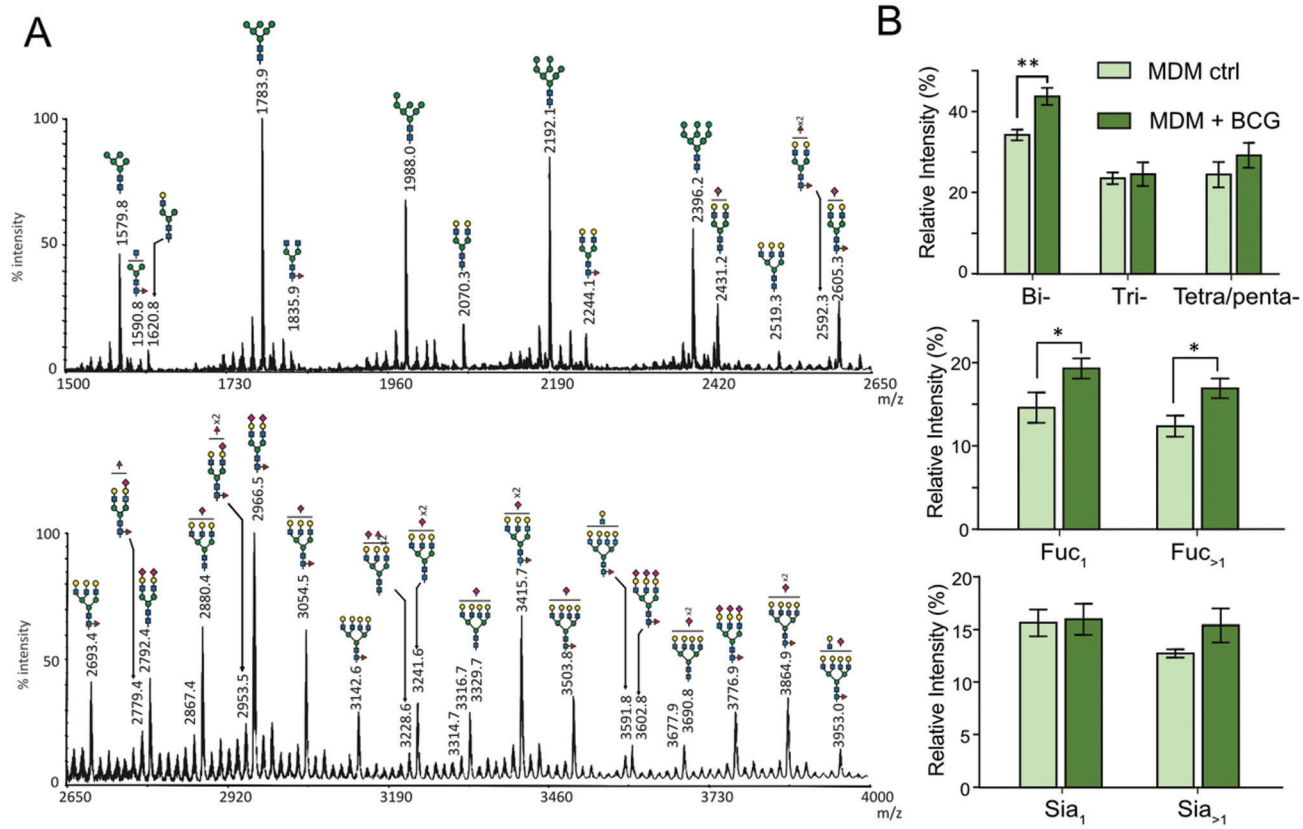

Fig. 3 Mass spectrometry analysis of *N*-glycans isolated from human MDM cells. (A) MALDI-MS profile of permethylated *N*-glycans purified from MDM cells. The top panel shows the *m/z* 1500 to 2650 region and the lower panel shows the *m/z* 2650 to 4000 region of a single MALDI-MS spectrum. The composition of major glycan signals was deduced from the *m/z* values of $[M + Na]^+$ adducts. The position of Fuc/Sia residues and branching patterns were not established at this stage and are indicative. A complete list of identified *N*-glycans is provided in the ESI,† Table S1. (B) Differential profiling of complex *N*-glycans before (light green) and after *M. bovis* BCG infection (dark green). Top, proportions of multi-antennary complex-type *N*-glycans (bi, two LacNAc; tri, three LacNAc; tetra/penta, four and five LacNAc); middle, proportions of mono and multi-fucosylated complex type *N*-glycans; bottom, proportions of sialylated *N*-glycan. Relative intensities do not include oligomannosylated *N*-glycans. The statistical significance compared with untreated cells (**$p < 0.01$, *$p < 0.05$) was determined by a two-tailed *t* test. Data represent median ± interquartile range from three independent experiments with different donors.

out based on the summed intensities of their respective diagnostic MS^2 ions (Fig. 4). The results indicated that Le^x was indeed more represented among the terminal glycotopes after BCG treatment. So was the core fucose as represented by the diagnostic MS^2 ion at *m/z* 468. Moreover, there was no significant amount of LacdiNAc or Le^y/Le^b (*m/z* 812), but a low level of sialyl fucosylated Hex-HexNAc (*m/z* 999) and diLacNAc (*m/z* 913) was detected.

The increased expression of cell-surface fucosylated epitope was further confirmed by flow cytometry using two fluorescent α1,3-fucose specific LTA and α1,2-fucose specific UEA-I lectins.[31,32] In agreement with MS analyses that showed an increased Le^x expression, LTA displays a higher binding on PMA-THP1 (×2.1) (Fig. 5A) and MDM (×4.5) (Fig. 5B) after infection ($p < 0{,}001$, $n = 3$). Inversely, the UEA signal associated with cells did not show any modification following infection. This recognition is carbohydrate-dependent, since fucose inhibits the LTA binding to cells (Fig. 5A and B, peaks 3).

Functional relevance

We have shown that infection by *M. bovis* BCG modifies the *N*-glycan patterns of the human macrophage PMA-THP-1 cell line and primary MDM. Most notably, we observed a modification in the average number of antennae and an increase in the surface expression of the Le^x antigen. On the contrary, activation by Pam_3Lp_{19}, an agonist of TLR2, increases the level of biantennary *N*-glycans but does not alter their fucosylation. This subtle difference suggests that mycobacterium-driven changes are not restricted to a TLR-2 dependent pathway. Our results are in agreement with Li and collaborators who suggested that only terminal and subterminal fucosylation, but not core fucosylation (linked α1,6), may be considered as a hallmark of M1 inflammatory macrophages.[33] Distinct human α(1,3)-fucosyltransferases (FUT) drive Lewis-X/sialyl Lewis-X assembly in human cells and some of them were predominately expressed during the inflammation process.[33,34] Furthermore, a decrease of fucose transcripts of fucosidase FUC1 in alveolar macrophages infected by *mycobacterium tuberculosis* has been previously described by Silver *et al.* in 2009.[16] Thus, it is not excluded that the gain of fucosylation observed in BCG-infected macrophages is induced by transcriptional or post-transcriptional regulation of theses enzymes. Moreover, the biosynthesis of the GDP-Fuc nucleotide or its intracellular transport in macrophages

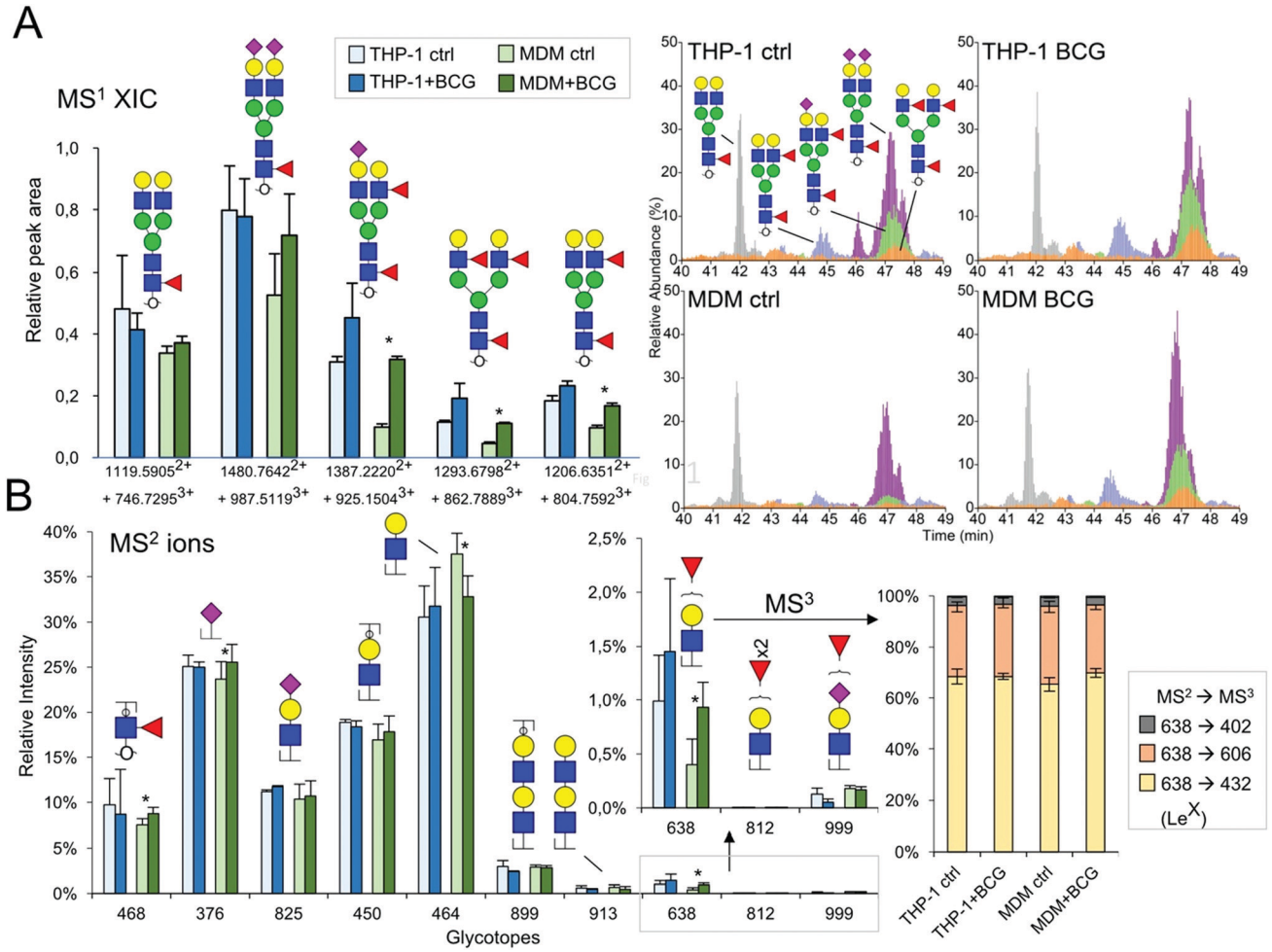

Fig. 4 LC-MS/MS analysis of macrophage *N*-glycans with and without BCG treatment. (A) The relative abundance of the five major sialylated and/or fucosylated biantennary *N*-glycans was inferred from extracted ion chromatogram plots (right panel, showing one set of data out of the three replicates) and relatively quantified based on their respective peak areas (left panel, averaged from 3 replicates, those of significance by statistical analysis are marked with *). The corresponding dataset from THP-1 cells is also plotted for side-by-side comparison. The relative peak areas were normalized to the Man_9 peak serving as an internal reference (taken as 1.0 in the bar chart, and 100% in the XIC plots). (B). The characteristic HCD MS^2 ions indicative of each of the annotated glycotopes were extracted from all MS^2 spectra acquired within the elution time of the *N*-glycans identified. Their respective ion intensities were summed and then calculated as the % total for comparative analysis purposes only and are not to be taken as true quantification. The charts for *m/z* 638, 812 and 999 (boxed) were magnified to show clearly the increase in *m/z* 638 for the MDM dataset. The THP-1 dataset was similarly plotted for comparison. Despite the significant increase in the fucosylated glycotope defined by *m/z* 638, the proportion that can be identified as LeX by its MS^3 ion at *m/z* 432 remained roughly constant. The MS^3 ion at *m/z* 606 is indicative of the H type 2 glycotope but may also be partly contributed by Le^x. A small amount of the MS^3 ion at *m/z* 402 suggests that a very low level of Le^a may also be present but the overall amount is negligible.

could be modified upon BCG infection, as previously reported in inflammation, tumorigenesis or apoptosis processes.[35,36] Fucosylated *N*-glycans also participate in tissue remodeling by reducing the activity of the tissue inhibitor of metalloproteinases-1 (TIMP-1).[37] Le^x is a stage specific embryonic antigen-1 (SSEA-1) and a marker for human myeloid cells that contributes to leukocyte recruitment to inflammatory sites by selectins and interacts with the immune receptor DC-SIGN. Several reports established that along differentiation and maturation of phagocytes, dynamic regulation of the expression of sLe^x and Le^x occurs, which may be due to transcriptional or post-translational changes of sialyltransferase and neuraminidase expression.[38] Indeed, both differentiation of monocytic THP-1 cells into macrophages and the maturation of DC reduce sLe^x expression at the cell surface.[22,39] The sLe^x epitope, expressed preferentially on molecules of monocytes such as PSGL1, CD43 and CD44, mediates the recruitment and adhesion of circulating leukocytes to the endothelium by interactions with *E*-selectin.[38]

Conclusion

In conclusion, we have directly identified and highlighted alterations in the *N*-glycome of human macrophages upon infection with *M. bovis* BCG, the most significant of which is the increased expression of the Le^x epitope. Further research is clearly needed to identify the spectrum of glycoproteins carrying the Le^x epitope and to determine how glycosylation changes are

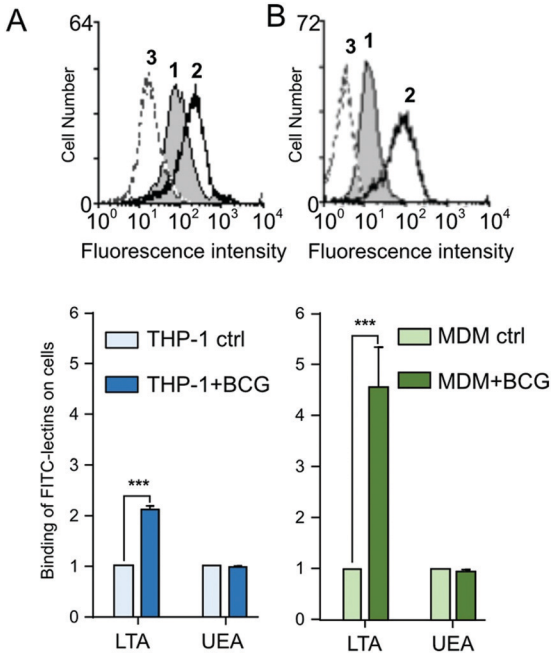

Fig. 5 Binding of plant lectins to macrophages THP-1 and MDM, after infection by *M. bovis* BCG: (A) PMA-THP1 and (B) MDM were infected by *M. bovis* BCG for 48 h and washed with PBS. FITC-conjugated LTA or UEA-I lectins that interact specifically with α L-fucose were incubated with untreated (ctrl) or stimulated cells, as described in the Method section. For each lectin, the mean fluorescence intensity (MFI) was determined by flow cytometry and the ratio MFI of infected cells *versus* MFI of untreated cells was determined. Binding of LTA lectin to unstimulated (grey peak 1) or to activated cells (peak 2) is illustrated in the fluorescence histograms. The addition of L-fucose to cells inhibits the LTA interaction with activated cells (peak 3). These data shown are representative of three independent experiments with similar results (***$p < 0.0001$).

driven by mycobacteria to promote infection. It is also needed to establish to what extent the modifications of the cell surface may impact host–pathogen interactions through mycobacterial lectins. Of particular interest, a ricin-type β-trefoil lectin, encoded by the *Rv1419* gene, has been detected in pleural effusions and granulomas of patients with active TB.[40] It modulates adhesion to murine and human derived macrophages and influences the intracellular growth of *Mtb*.[41] Finally, changes in fucose metabolism could be analyzed by click-chemistry in BCG-infected macrophages using GDP-FucAz. The effect of the 6-alkinyl-fucose inhibitor on macrophage infection by mycobacteria should also be investigated.

Abbreviations

DC-SIGN	Dendritic cell-specific ICAM-grabbing non-integrin
GTs	Glycosyltransferases
GSL	Glycosphingolipids
GM-CSF	Granulocyte-macrophage colony stimulating factor
LTA	Lotus tetranologobus agglutinin
MS	Mass spectrometry
MDM	Monocyte-derived macrophages
M.	Mycobacterium
Mtb	*Mycobacterium tuberculosis*
NG	*N*-Glycans
PMA	Phorbol-12-myristate-13-acetate
TLR	Toll-like receptors
TDM	Trehalose-diMycolate
SIGLECS	Sialic acid binding Ig-like lectins
SSEA-1	Stage specific embryonic antigen-1
UEA-I	Ulex europaeus I agglutinin

Conflicts of interest

There are no conflicts to declare.

Acknowledgements

The work was supported by the Ministère de l'Enseignement Supérieur et de la Recherche (to CD), by a VisonnAIRR grant from Région Hauts-de-France (to DM), and an Academia Sinica Investigator Award grant AS-IA-105-L02 (to KHK). We are grateful to Marlène Mortuaire for technical advice in cell culture. We are indebted to the Research Federation FRABio (Univ. Lille, CNRS, FR 3688, FRABio, Biochimie Structurale et Fonctionnelle des Assemblages Biomoléculaires) and to the PAGés platform (http://plateforme-pages.univ-lille1.fr) for providing the scientific and technical environment conducive to achieving this work. We further acknowledge LC-MS/MS data acquisition at the Academia Sinica Common Mass Spectrometry Facilities for Proteomics and Protein Modification Analysis located at the Institute of Biological Chemistry, Academia Sinica, supported by the Academia Sinica Core Facility and Innovative Instrument Project (AS-CFII-108-107).

Notes and references

1 K. W. Moremen, M. Tiemeyer and A. V. Nairn, Vertebrate protein glycosylation: diversity, synthesis and function, *Nat. Rev. Mol. Cell Biol.*, 2012, **13**(7), 448–462.
2 H. J. F. Maccioni, R. Quiroga and W. Spessott, Organization of the synthesis of glycolipid oligosaccharides in the Golgi complex, *FEBS Lett.*, 2011, **585**(11), 1691–1698.
3 S. S. Pinho and C. A. Reis, Glycosylation in cancer: mechanisms and clinical implications, *Nat. Rev. Cancer*, 2015, **15**(9), 540–555.
4 G. A. Rabinovich, Y. van Kooyk and B. A. Cobb, Glycobiology of immune responses, *Ann. N. Y. Acad. Sci.*, 2012, **1253**, 1–15.
5 J. L. Johnson, M. B. Jones, S. O. Ryan and B. A. Cobb, The regulatory power of glycans and their binding partners in immunity, *Trends Immunol.*, 2013, **34**(6), 290–298.
6 A. C. Semel, E. C. Seales, A. Singhal, E. A. Eklund, K. J. Colley and S. L. Bellis, Hyposialylation of integrins stimulates the activity of myeloid fibronectin receptors, *J. Biol. Chem.*, 2002, **277**(36), 32830–32836.

7 Y. Su, T. Bakker, J. Harris, C. Tsang, G. D. Brown and M. R. Wormald, *et al.*, Glycosylation influences the lectin activities of the macrophage mannose receptor, *J. Biol. Chem.*, 2005, **280**(38), 32811–32820.
8 H. Kataoka, M. Yasuda, M. Iyori, K. Kiura, M. Narita and T. Nakata, *et al.*, Roles of N-linked glycans in the recognition of microbial lipopeptides and lipoproteins by TLR2, *Cell. Microbiol.*, 2006, **8**(7), 1199–1209.
9 B. L. Schulz, A. J. Sloane, L. J. Robinson, S. S. Prasad, R. A. Lindner and M. Robinson, *et al.*, Glycosylation of sputum mucins is altered in cystic fibrosis patients, *Glycobiology*, 2007, **17**(7), 698–712.
10 M. Barel, A. Harduin-Lepers, L. Portier, M.-C. Slomianny and A. Charbit, Host glycosylation pathways and the unfolded protein response contribute to the infection by *Francisella*: Glycosylation and UPR in Francisella infection, *Cell. Microbiol.*, 2016, **18**(12), 1763–1781.
11 N. J. Hare, L. Y. Lee, I. Loke, W. J. Britton, B. M. Saunders and M. Thaysen-Andersen, Mycobacterium tuberculosis Infection Manipulates the Glycosylation Machinery and the N-Glycoproteome of Human Macrophages and Their Microparticles, *J. Proteome Res.*, 2017, **16**(1), 247–263.
12 A. Magalhães, R. Marcos-Pinto, A. V. Nairn, M. Dela Rosa, R. M. Ferreira and S. Junqueira-Neto, *et al.*, Helicobacter pylori chronic infection and mucosal inflammation switches the human gastric glycosylation pathways, *Biochim. Biophys. Acta*, 1852, **9**, 1928–1939.
13 M. J. Marakalala, F. O. Martinez, A. Plüddemann and S. Gordon, Macrophage Heterogeneity in the Immunopathogenesis of Tuberculosis, *Front. Microbiol.*, 2018, **9**, 1028.
14 P. Sampath, K. Moideen, U. D. Ranganathan and R. Bethunaickan, Monocyte Subsets: Phenotypes and Function in Tuberculosis Infection, *Front. Immunol.*, 2018, **9**, 1726.
15 M. da Silva Siqueira, R. de Moraes Ribeiro and L. H. Travassos, Autophagy and Its Interaction With Intracellular Bacterial Pathogens, *Front. Immunol.*, 2018, **9**, 935.
16 R. F. Silver, J. Walrath, H. Lee, B. A. Jacobson, H. Horton and M. R. Bowman, *et al.*, Human alveolar macrophage gene responses to Mycobacterium tuberculosis strains H37Ra and H37Rv, *Am. J. Respir. Cell Mol. Biol.*, 2009, **40**(4), 491–504.
17 D. Kumar, L. Nath, M. A. Kamal, A. Varshney, A. Jain and S. Singh, *et al.*, Genome-wide analysis of the host intracellular network that regulates survival of Mycobacterium tuberculosis, *Cell*, 2010, **140**(5), 731–743.
18 A. M. Mercurio, G. A. Schwarting and P. W. Robbins, Glycolipids of the mouse peritoneal macrophage. Alterations in amount and surface exposure of specific glycolipid species occur in response to inflammation and tumoricidal activation, *J. Exp. Med.*, 1984, **160**(4), 1114–1125.
19 S. Afroun, J. P. Tenu and G. Lemaire, Modifications of glycosylation patterns in macrophages upon activation, *Biochim. Biophys. Acta*, 1988, **971**(2), 137–147.
20 E. Mendoza-Coronel and M. Castañón-Arreola, Comparative evaluation of in vitro human macrophage models for mycobacterial infection study, *Pathog. Dis.*, 2016, **74**(6), ftw052.
21 W. Chanput, J. J. Mes and H. J. Wichers, THP-1 cell line: An in vitro cell model for immune modulation approach, *Int. Immunopharmacol.*, 2014, **23**(1), 37–45.
22 C. P. Delannoy, Y. Rombouts, S. Groux-Degroote, S. Holst, B. Coddeville and A. Harduin-Lepers, *et al.*, Glycosylation Changes Triggered by the Differentiation of Monocytic THP-1 Cell Line into Macrophages, *J. Proteome Res.*, 2017, **16**(1), 156–169.
23 S. Tsuchiya, Y. Kobayashi, Y. Goto, H. Okumura, S. Nakae and T. Konno, *et al.*, Induction of maturation in cultured human monocytic leukemia cells by a phorbol diester, *Cancer Res.*, 1982, **42**(4), 1530–1536.
24 A. Ohradanova-Repic, C. Machacek, M. B. Fischer and H. Stockinger, Differentiation of human monocytes and derived subsets of macrophages and dendritic cells by the HLDA10 monoclonal antibody panel, *Clin. Transl. Immunol.*, 2016, **5**(1), e55.
25 M. H. Larsen, K. Biermann and W. R. Jacobs, Laboratory maintenance of Mycobacterium tuberculosis, *Curr. Protoc. Microbiol.*, 2007, **10**, 10A.1.
26 A. B. Schromm, N. Reiling, J. Howe, K.-H. Wiesmüller, M. Roessle and K. Brandenburg, Influence of serum on the immune recognition of a synthetic lipopeptide mimetic of the 19 kDa lipoprotein from Mycobacterium tuberculosis, *Innate Immun.*, 2010, **16**(4), 213–225.
27 C. J. Riendeau and H. Kornfeld, THP-1 cell apoptosis in response to Mycobacterial infection, *Infect. Immun.*, 2003, **71**(1), 254–259.
28 I. Ciucanu and F. Kerek, A simple and rapid method for the permethylation of carbohydrates, *Carbohydr. Res.*, 1984, **131**(2), 209–217.
29 C.-T. Hsiao, P.-W. Wang, H.-C. Chang, Y.-Y. Chen, S.-H. Wang and Y. Chern, *et al.*, Advancing a High Throughput Glycotope-centric Glycomics Workflow Based on nanoLC-MS^2-product Dependent-MS^3 Analysis of Permethylated Glycans, *Mol. Cell. Proteomics*, 2017, **16**(12), 2268–2280.
30 K. Jiang, H. Zhu, L. Li, Y. Guo, E. Gashash and C. Ma, *et al.*, Sialic acid linkage-specific permethylation for improved profiling of protein glycosylation by MALDI-TOF MS, *Anal. Chim. Acta*, 2017, **981**, 53–61.
31 S. Sughii, E. A. Kabat and H. H. Baer, Further immunochemical studies on the combining sites of Lotus tetragonolobus and Ulex europaeus I and II lectins, *Carbohydr. Res.*, 1982, **99**(1), 99–101.
32 L. Yan, P. P. Wilkins, G. Alvarez-Manilla, S. I. Do, D. F. Smith and R. D. Cummings, Immobilized Lotus tetragonolobus agglutinin binds oligosaccharides containing the Le(x) determinant, *Glycoconjugate J.*, 1997, **14**(1), 45–55.
33 J. Li, H.-C. Hsu, Y. Ding, H. Li, Q. Wu and P. Yang, *et al.*, Inhibition of Fucosylation Reshapes Inflammatory Macrophages and Suppresses Type II Collagen-Induced Arthritis: Inhibition of Fucosylation in Arthritis, *Arthritis Rheumatol.*, 2014, **66**(9), 2368–2379.
34 N. Mondal, B. Dykstra, J. Lee, D. J. Ashline, V. N. Reinhold and D. J. Rossi, *et al.*, Distinct human α(1,3)-fucosyltransferases drive Lewis-X/sialyl Lewis-X assembly in human cells, *J. Biol. Chem.*, 2018, **293**(19), 7300–7314.

35 J. Niittymäki, P. Mattila and R. Renkonen, Differential gene expression of GDP-L-fucose-synthesizing enzymes, GDP-fucose transporter and fucosyltransferase VII, *APMIS*, 2006, **114**(7–8), 539–548.

36 K. Moriwaki, M. Narisada, T. Imai, S. Shinzaki and E. Miyoshi, The effect of epigenetic regulation of fucosylation on TRAIL-induced apoptosis, *Glycoconjugate J.*, 2010, **27**(7–9), 649–659.

37 H. I. Kim, R. Saldova, J. H. Park, Y. H. Lee, D. J. Harvey and M. R. Wormald, *et al.*, The presence of outer arm fucose residues on the N-glycans of tissue inhibitor of metallo-proteinases-1 reduces its activity, *J. Proteome Res.*, 2013, **12**(8), 3547–3560.

38 Z. Silva, Z. Tong, M. Guadalupe Cabral, C. Martins, R. Castro and C. Reis, *et al.*, Sialyl Lewisx-dependent binding of human monocyte-derived dendritic cells to selectins, *Biochem. Biophys. Res. Commun.*, 2011, **409**(3), 459–464.

39 S. Julien, M. J. Grimshaw, M. Sutton-Smith, J. Coleman, H. R. Morris and A. Dell, *et al.*, Sialyl-Lewis(x) on P-selectin glycoprotein ligand-1 is regulated during differentiation and maturation of dendritic cells: a mechanism involving the glycosyltransferases C2GnT1 and ST3Gal I, *J. Immunol.*, 2007, **179**(9), 5701–5710.

40 L. Nogueira, F. C. Cardoso, A. M. Mattos, J. Bordignon, C. P. Figueiredo and P. Dahlstrom, *et al.*, Mycobacterium tuberculosis Rv1419 encodes a secreted 13 kDa lectin with immunological reactivity during human tuberculosis, *Eur. J. Immunol.*, 2010, **40**(3), 744–753.

41 A. Bafica, S. Morales, C. Eto, N. Souza, L. Nogueira and L. Riley, *et al.*, A mycobacterial lectin promotes bacilli adhesion to macrophages and influences pathogen growth during infection (INM3P.409), *J. Immunol.*, 2015, **194**(suppl 1), 127.14.

42 A. Varki, R. D. Cummings, M. Aebi, N. H. Packer, P. H. Seeberger and J. D. Esko, *et al.*, Symbol Nomenclature for Graphical Representations of Glycans, *Glycobiology*, 2015, **25**(12), 1323–1324.

